trations to cause similar inhibition. In contrast, the observed product of the methylreductase reaction, HS-CoM (**1**), does not cause measurable levels of inhibition of methanogenesis up to a concentration of 10 mM. This would indicate that the rate of methane formation in the routine reductase assay is not influenced by the accumulation of HS-CoM over the time course of the assay.

The disulfide form of the cofactor, $(S\text{-}CoM)_2$ (**9**), causes noticeable inhibition in the mM range (Figure 3). Extracts of *M. thermoautotrophicum* catalyze the reduction of the disulfide, and CoM was observed to exist in the reduced form in active extracts. The inhibition observed for $(S\text{-}CoM)_2$ may be due to competition between $(S\text{-}CoM)_2$ reductase and methyl-CoM reductase for reducing equivalents from molecular hydrogen or due to the accumulation of HS-CoM.

Results of experiments in which other analogues were tested for their ability to inhibit methane formation from CH_3-S-CoM indicated that CH_3CH_2-S-CoM (**7**) and $CH_3CH_2CH_2$-S-CoM (**8**) caused only 50% inhibition at the high ratio of analogue to CH_3-S-CoM of 17 and 22, respectively. When the following analogues were tested at a ratio of analogue to CH_3-S-CoM of 100, no inhibition of methylreductase was detected: $HO(CH_2)_2SO_3^-$; $H_2N(CH_2)_2SO_3^-$; $CH_3NH(CH_2)_2SO_3^-$; $^-O_3S(CH_2)_2SO_3^-$; $CH_3S(CH_2)_2OH$. When CH_3-S-CoM was added at the same concentration (5×10^{-2} M), no inhibition in the rate of methane formation was observed.

With the potent inhibitors, $BrCH_2CH_2SO_3^-$ and $ClCH_2CH_2SO_3^-$, inhibition of the methyl reductase is not reversed when the substrate concentration of CH_3-S-CoM is increased 100-fold. The precise definition and quantitation of the mode by which these inhibitors act must await resolution and purification of the components involved in methanogenesis.

Acknowledgments

We appreciate the assistance of Paquita Erazo and Robert Mangoff in the synthesis of CoM analogues and of Victor Gabriel in the culture of the organism.

References

Ellman, G. (1959) *Arch. Biochem. Biophys. 82*, 70-77.
Gunsalus, R. P., & Wolfe, R. S. (1977) *Biochem. Biophys. Res. Commun. 76*, 790-795.
Hungate, R. E. (1969) *Methods Microbiol. 3B*, 117-132.
McBride, B. C., & Wolfe, R. S. (1971) *Biochemistry 10*, 2317-2324.
Schramm, C. H., Lemaire, H., & Karlson, R. H. (1955) *J. Am. Chem. Soc. 77*, 6231-6233.
Taylor, C. D., & Wolfe, R. S. (1974a) *J. Biol. Chem. 249*, 4879-4885.
Taylor, C. D., & Wolfe, R. S. (1974b) *J. Biol. Chem. 249*, 4886-4890.
Zeikus, J. G., & Wolfe, R. S. (1972) *J. Bacteriol. 109*, 707-713.

Distribution of Ultraviolet-Induced DNA Repair Synthesis in Nuclease Sensitive and Resistant Regions of Human Chromatin†

Michael J. Smerdon,‡ Thea D. Tlsty,§ and Michael W. Lieberman*

ABSTRACT: The distribution of ultraviolet radiation (UV) induced DNA repair synthesis within chromatin was examined in cultured human diploid fibroblasts (IMR-90). Measurement of the time course of repair synthesis yielded two distinct phases: An initial rapid phase (fast repair) which occurs during the first 2-3 h after damage and a slower phase (slow repair) associated with a tenfold decrease in the rate of nucleotide incorporation, which persists for at least 35 h after damage. Staphylococcal nuclease digests of nuclei from cells damaged with UV and labeled during the fast-repair phase revealed a marked preference of fast-repair synthesis for the nuclease-sensitive regions. A new method was developed to analyze the digestion data and showed that approximately 50% of the nucleotides incorporated during the fast-repair phase are located in staphylococcal nuclease-sensitive regions, which comprise about 30% of the genome. Calculations from these data indicate that in the staphylococcal nuclease-sensitive regions the number of newly inserted nucleotides per unit DNA is about twice that of resistant regions. These results were supported by electrophoresis studies which demonstrated a decreased representation of fast-repair synthesis in core particle DNA. In contrast, the distribution within chromatin of nucleotides incorporated during the slow-repair phase was found to be much more homogeneous with about 30% of the repair sites located in 25% of the genome. Digestion studies with DNase I indicated a slight preference of repair synthesis for regions sensitive to this enzyme; however, no marked difference between the distributions of fast- and slow-repair synthesis was observed. This study provides evidence that the structural constraints placed upon DNA in chromatin also place constraints upon UV-induced DNA repair synthesis in human cells.

Although recent studies have greatly increased our understanding of chromatin structure (Hewish and Burgoyne, 1973; Woodcock, 1973; Olins and Olins, 1973, 1974; Sahasrabudde and Van Holde, 1974; Kornberg, 1974; Noll, 1974), to date there have been relatively few studies dealing with the role of chromatin structure in *excision repair* (Ramanathan et al.,

† From the Department of Pathology, Washington University School of Medicine, St. Louis, Missouri 63110. *Received December 12, 1977.* This study was supported by grants from the National Institutes of Health (CA-16217; CA-20513; RR-05389). This study was also supported by the following companies: Brown & Williamson Tobacco Corp.; Larus and Brother Co., Inc.; Liggett & Myers, Inc.; Lorillard, a Division of Loews Theatres, Inc.; Philip Morris, Inc.; R. J. Reynolds Tobacco Co.; United States Tobacco Co.; and Tobacco Associates, Inc.

‡ Recipient of a National Institutes of Health postdoctoral fellowship (CA-09118).

§ Recipient of a National Institutes of Health predoctoral fellowship (ES-00128).

0006-2960/78/0417-2377$01.00/0

1976; Bodell, 1977; Cleaver, 1977; for reviews on excision repair, see: Beers et al., 1972; Cleaver, 1974; Hanawalt and Setlow, 1975; Lieberman, 1976; Nichols and Murphy, 1977). Clearly, such studies are of interest since the constraints placed upon DNA by chromatin structure may place constraints upon the repair process. Evidence to date indicates that much of the methodology which has been developed to probe chromatin structure is applicable to the study of *repair synthesis* within chromatin. Nuclease digestion studies have played a central role in the analysis of chromatin structure. The following observations allow the extension of this approach to the analysis of the distribution of repair synthesis within chromatin: During repair synthesis nucleotides are inserted by a template-directed process and, at least by physicochemical techniques, are indistinguishable from the rest of the genome (Lieberman and Poirier, 1974c; Lieberman, 1976); the sequence complexity of DNA does not appear to be related to the distribution of repair synthesis (Meltz and Painter, 1973; Lieberman and Poirier, 1974a,b; Drahovsky et al., 1976). Using staphylococcal nuclease and DNase I, which are sensitive to different structural constraints within chromatin (Axel et al., 1975; Lacy and Axel, 1975; Weintraub and Groudine, 1976; Simpson and Whitlock, 1976; Keichline et al., 1976; Garel and Axel, 1976; Levy and Dixon, 1977), we have studied the effect of chromatin structure on the distribution of DNA repair synthesis in cultured human diploid fibroblasts damaged with ultraviolet radiation (UV) and the relation of the time course of repair synthesis to this distribution.

Materials and Methods

Cell Culture and Preparation of Prelabeled Cells (*Replicative Synthesis*). Human diploid fibroblasts (IMR-90 cells; passages 12–22; Nichols et al., 1977) were grown as previously described (Amacher et al., 1977). Thirty-six to 48 h after the cells were split (generally 1:3), 0.05 μCi/mL (final concentration) [^{14}C]thymidine (New England Nuclear; 50–60 mCi/mmol) was added to the medium for 20 to 40 h. The medium was then replaced with fresh medium (without [^{14}C]thymidine). To prepare cells with both [^{14}C]- and [^{3}H]thymidine incorporated during replication, the replacement medium contained 0.1 μCi/mL (final concentration) [^{3}H]thymidine (New England Nuclear; 50–60 Ci/mmol). After 20 h, this medium was replaced, and the cells were allowed to grow to confluence.

Repair Experiments. All irradiation and labeling operations were performed in a warm room at 35–37 °C. The dishes were then placed in a NAPCO CO_2 incubator until harvested.

UV Irradiation and [^{3}H]*Thymidine Labeling* (*Repair Synthesis*). Confluent cells, prelabeled with [^{14}C]thymidine, were treated with 10 mM hydroxyurea (Sigma) prior to UV irradiation as previously described (Lieberman and Poirier, 1973). The medium was removed and the cells were irradiated with a 15-W germicidal lamp (predominantly 254 nm) with a flux of 2.0 W/m^2 and a total dose of 12 J/m^2. The medium was replaced and 10 μCi/mL (final concentration) [^{3}H]thymidine was added. Cells treated identically with the omission of the irradiation step served as a control and provided data for the estimation of σ (see Results and Appendix).

UV Irradiation and [^{3}H]*Bromodeoxyuridine Labeling* (*Repair Synthesis*). Confluent cells (not prelabeled with [^{14}cO]thymidine or treated with hydroxyurea) were labeled with [^{3}H]bromodeoxyuridine (BrdUrd) by using a modification of the method of Smith and Hanawalt (1976a,b). Prior to irradiation, 10^{-5} M BrdUrd (Sigma)(final concentration) and 5 μCi/mL (final concentration) [^{3}H]BrdUrd (New England Nuclear; 22 Ci/mmol) were added to the medium. After 1 h, the medium was removed and the cells were irradiated as described above. The medium was then replaced.

Preparation of Nuclei for Nuclease Digestions. Cells were collected by scraping, followed by centrifugation in 0.15 M NaCl at 600*g* for 10 min at 2 °C. The cell pellet was washed in ice-cold digestion buffer (10 mM Tris,[1] pH 8, 0.1 mM $CaCl_2$, and 0.25 M sucrose), and repelleted at 16 000*g* for 10 min. The cells were lysed, and the nuclei were recovered by vortexing the cell pellet in digestion buffer and 0.5% Triton X-100, followed by centrifugation (16 000*g* for 10 min). The lysing step was repeated two more times, and the nuclei were washed with digestion buffer and pelleted by centrifugation (16 000*g* for 10 min). The wash step was repeated, and the nuclear pellet was resuspended in digestion buffer by gentle dounce homogenization (Kontes; B pestle).

Preparation of Naked DNA for Nuclease Digestions. DNA was prepared from an aliquot of the final nuclear suspension as previously described (Lieberman and Dipple, 1972), except that the CsCl centrifugation step was modified: A 4.2-mL aliquot was centrifuged at 54 000 rpm to equilibrium at 25 °C in a Sorvall TV865 vertical rotor. After the gradient was fractionated and the peak fractions were dialyzed (10 mM Tris, pH 8.0; 0.1 mM $CaCl_2$), the absorbance spectrum was measured (Gilford 250 spectrometer equipped with wavelength scanner and recorder) and always gave an A_{230}/A_{260} ratio of 0.42–0.44 and an A_{260}/A_{280} ratio of 1.77–1.79. Before digestion with nuclease, the DNA solution was adjusted to 10 mM Tris (pH 8), 0.1 mM $CaCl_2$, and 0.25 M sucrose by the addition of sucrose in 10 mM Tris (pH 8) and 0.1 mM $CaCl_2$.

Nuclease Digestions. Suspended nuclei (~30 μg/mL DNA) or DNA (~20 μg/mL) was digested by staphylococcal nuclease (Worthington; 11.6 units/μg) or bovine pancreatic DNase I (Sigma; 3260 Kunitz units/mg) in digestion buffer at 37 °C. Enzyme concentrations of 0.4–2.0 μg/mL (depending on the experiment) were used in digestions of nuclei and 0.04 μg/mL in digestions of DNA. At time zero, the nuclease was added. At various times during the digestion, a 0.25-mL aliquot of the reaction mixture was transferred to a tube containing 0.025 mL of 0.1 M EDTA (pH 7) on ice and vortexed, terminating the reaction. Ice-cold 70% PCA (0.03 mL) was then added, and the tube was vortexed. After 20 min at 0 °C, samples were centrifuged at 16 000*g* for 10 min. A 0.2-mL aliquot of the 7% PCA supernatant was then diluted to 1 mL with H_2O and counted in 6 mL of Insta Gel (Packard) in a Beckman LS-333 liquid scintillation spectrometer. The ^{14}C overlap in the ^{3}H channel was determined by counting [^{14}C]thymidine under identical solution conditions. The ^{3}H counts were then determined by using the standard double-label equations (Kobayashi and Maudsley, 1974; Horrocks, 1974).

To determine the 100% digestion value, an aliquot of the suspended nuclei was first digested with proteinase K (EM Laboratories) at a concentration of 20 μg/mL for 2 h at 37 °C. Two aliquots of this solution, one containing 50 μg/mL DNase I and the other containing 50 μg/mL staphylococcal nuclease, were then incubated at 37 °C. A third aliquot was incubated with 7% PCA at 70 °C. Aliquots of each of these samples were taken at 0.5, 1, 1.5, 2, and 2.5 h after the addition of nuclease or PCA. The aliquots from the nuclease samples were precipitated in ice-cold 7% PCA as described above. All three sets of aliquots were then centrifuged and the supernatants were counted. In each case the amount of radioactivity was constant

[1] Abbreviations used are: Tris, 2-amino-2-hydroxymethyl-1,3-propanediol; EDTA, (ethylenedinitrilo)tetraacetic acid.

with time after 0.5 h for staphylococcal nuclease digestions and after 1.5 h for DNase I and 7% PCA digestions. The addition of nuclease at 2 h did not change the 2.5-h values. The 100% digestion values obtained from each method always agreed to within 3%. We note that in these studies the same results were obtained when nuclease was added either directly to the proteinase K digested samples or after heating the samples to 100 °C for 5 min. This observation and the results obtained from 7% PCA digestions indicate that under these conditions the protease did not affect the nuclease action.

Preparation of [^{3}H]BrdUrd Labeled DNA. DNA was prepared and banded in CsCl gradients by the method of Smith and Hanawalt (1976a,b) with some modification. Cells were collected and lysed as described above. The nuclear pellet was washed once with 10 mM Tris (pH 8), 10 mM EDTA, 10 mM NaCl and digested overnight at 37 °C with 150 μg/mL proteinase K in the above solution containing 0.1% $NaDodSO_4$. The solution was then brought to a density of 1.72 g/cm^3 with CsCl and a final volume of 8 mL and centrifuged at 8000*g*. The clear phase was collected and centrifuged in polycarbonate tubes at 37 000 rpm at 20 °C for 36 h. The gradients were fractionated, and the A_{260} and radioactivity were measured as described above. The fractions across the light peak were then pooled and added to 0.7 mL of 1 M K_2HPO_4, pH 12.5. This solution was brought to a final volume of 7 mL and a density of 1.76 g/cm^3 with H_2O and CsCl. The solution (overlayered with paraffin oil) was centrifuged in polyallomer tubes at 37 000 rpm at 20 °C for 36 h. The gradients were fractionated, and the A_{260} and radioactivity were measured as described above.

Electrophoresis. Samples were prepared by taking 0.5-mL aliquots of the nuclear digestion, adding 0.05 mL of 0.1 M EDTA (pH 7), and incubating with100 μg/mL proteinase K at 37 °C for at least 12 h. The DNA was precipitated with ethanol and the precipitates were dissolved in 0.1 × E buffer (E buffer consists of 40 mM Tris, pH 7.4, 20 mM sodium acetate, 1.1 mM EDTA). Electrophoresis was carried out on horizontal 2.8% agarose (Sea Kem) slab gels (13 × 25 cm) in E buffer. Gels were run for 7-8 h at 100 V, stained in 2 μg/mL ethidium bromide, illuminated (Ultra-Violet Products, Inc., transilluminator), and photographed through a red filter with Polaroid Type 55 film. Slices of the gel (2 mm) were transferred to glass scintillation vials. After the addition of 2 mL of H_2O to each vial, the gel slices were solubilized by heating. Once cooled, the samples were counted in 12 mL of Insta Gel. The sizes of the digestion products were determined by coelectrophoresis with *Hae*III restriction fragments of PM2 DNA, which were the generous gift of Drs. R. T. Kovacic and K. E. Van Holde. The sizes of the restriction fragments used in this paper are those given in Kovacic and Van Holde (1977).

Results

Time Course of Repair Synthesis after UV. We have measured the time dependence of repair synthesis in confluent human fibroblasts by three different methods. The first method utilized [^{3}H]thymidine (dThd) as the label and the DNA was purified on neutral CsCl gradients (Lieberman and Poirier, 1973). The difference in specific activities between the DNA from UV-irradiated cells and the DNA from control cells was used as a measure of repair synthesis. Replicative synthesis was suppressed to very low levels in these cells by contact inhibition (confluence) and hydroxyurea. The second method used the density label bromodeoxyuridine (BrdUrd) to measure repair synthesis. In these experiments no hydroxyurea was present. DNA from UV-damaged cells, which were allowed to repair

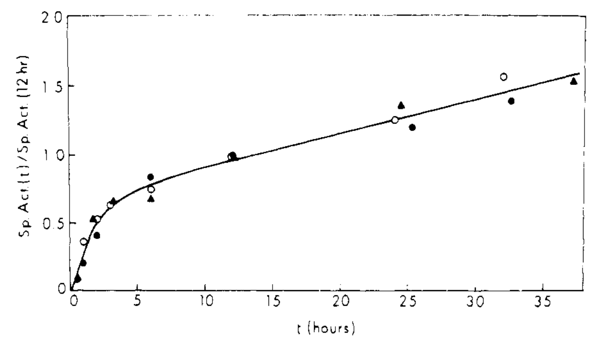

FIGURE 1: Time course of repair synthesis. Confluent cells were irradiated with 12 J/m^2 UV at time zero, and the amount of repair synthesis was measured by one of three methods: Method 1 (●) consisted of labeling both damaged and undamaged (control) cells for the indicated times in the presence of hydroxyurea and [^{3}H]dThd, purifying the DNA on neutral CsCl gradients (see Materials and Methods), and measuring the difference in specific activities between DNA from UV-treated cells and DNA from control cells. Method 2 (○) consisted of labeling cells in the presence of [^{3}H]BrdUrd, banding the DNA in a neutral CsCl gradient, followed by a reband of the light DNA peak in an alkaline CsCl gradient, and measuring the specific activity of the light peak in the second gradient. Method 3 (▲) consisted of prelabeling cells with [^{14}C]dThd during the log phase of growth and labeling both damaged and control cells with [^{3}H]dThd in the presence of hydroxyurea (see Materials and Methods). Nuclei were prepared and incubated at 37 °C with proteinase K (20 μg/mL) for 12 h and then staphylococcal nuclease (20 μg/mL) for 4 h, and values were obtained by measuring the difference in ^{3}H to ^{14}C ratios between the damaged and control samples. Data are presented as the specific activity at time *t* normalized to the specific activity at 12 h. The 12-h specific activity was 7375 cpm/μg for method 1, 153.5 cpm/μg for method 2, and 1.59 (^{3}H cpm/^{14}C cpm) for method 3.

in the presence of [^{3}H]BrdUrd, was banded in a neutral CsCl gradient, and the light density peak was pooled and rebanded in an alkaline CsCl gradient (Smith and Hanawalt, 1976a,b). The specific activity of the DNA in the light peak of the second gradient is a measure of the amount of repair synthesis. The third method is similar to the first in that [^{3}H]dThd was used as the label and hydroxyurea was present; however, these cells were prelabeled during replicative synthesis with [^{14}C]dThd. Nuclei prepared from these cells were first digested with proteinase K followed by digestion with staphylococcal nuclease and then counted. The difference in ^{3}H to ^{14}C ratios between the DNA from damaged cells and the DNA from control cells was used as the measure of repair synthesis. The results of each of these methods normalized to their respective 12-h values are shown in Figure 1.

The data from all three methods indicate that repair synthesis in normal human diploid fibroblasts damaged with UV may be divided into at least two different phases: An initial, rapid phase occurs during the first 2-3 hours ("fast repair"), and a slower phase, the onset of which cannot be determined accurately, continues for at least 35 h ("slow repair").[2] The ratio of the initial and final slopes for the curve shown is 12. Thus, on a unit DNA basis, nucleotides are inserted approximately 12-fold more rapidly during fast repair than during slow repair. These large differences in nucleotide incorporation rate cannot be accounted for by isotope dilution (utilization of a significant fraction of the labeled pool) because addition of [^{3}H]BrdUrd at 8 h after damage instead of at time 0 resulted in at most a 20% increase in incorporation rate during slow repair (method 2; data not shown).

These results suggested to us that the distribution of UV-

[2] The terms "fast repair" and "slow repair" are used *only* as an aid in referring to the two regions in Figure 1 differing in nucleotide incorporation rate and are not intended to imply molecular mechanisms.

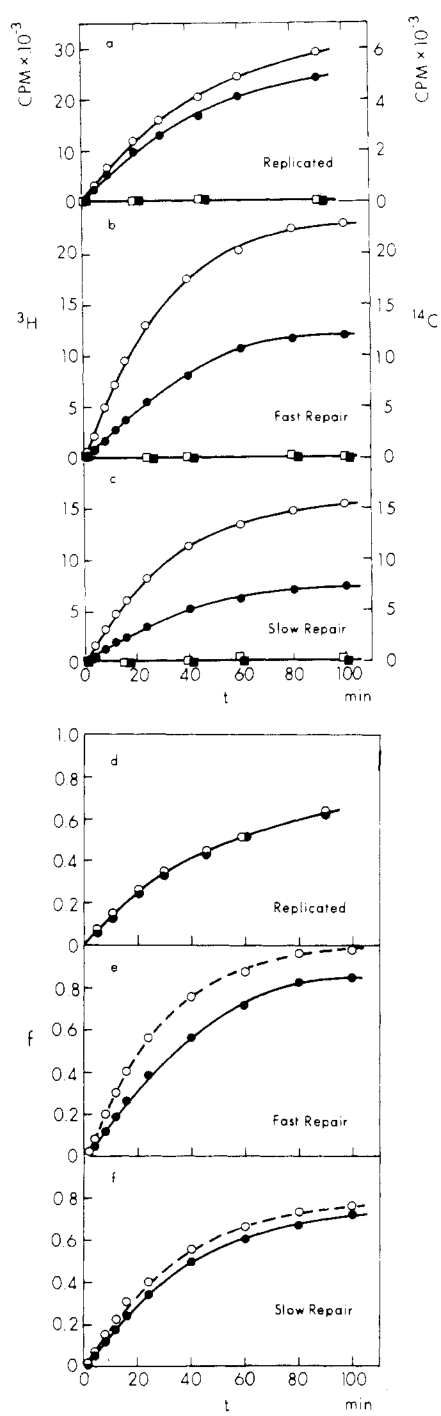

FIGURE 2: Staphylococcal nuclease digestion kinetics for nuclei labeled during replication, fast repair, and slow repair. Data are plotted as release of acid-soluble cpm (a–c) and fraction (f) of total cpm (d–f) as a function of time of incubation (0.4 μg/mL staphylococcal nuclease and 25–30 μg/mL DNA-chromatin as nuclei). Panels a and d represent data from cells labeled with [^{14}C]dThd (●) and [^{3}H]dThd (○) during replicative synthesis; panels b and e represent data from cells prelabeled with [^{14}C]dThd (●) and labeled during fast-repair synthesis (0–3 h) with [^{3}H]dThd (○); panels c and f represent data from cells prelabeled with [^{14}C]dThd (●) and labeled during slow-repair synthesis (12–29 h) with [^{3}H]dThd (○). ^{3}H cpm (□) and ^{14}C cpm (■) released from nuclei incubated in the absence of nuclease are shown in each case (a–c).

TABLE I: Kinetic Data Analyses.[a]

Repair	Expt	σ	ξ	f_S	f_R	Sum test
		A. Staphylococcal Nuclease Digests				
Fast	1	42	0.32	0.52	0.49	1.01
Fast	2	54	0.32	0.48	0.58	1.06
Fast	3	38	0.33	0.45	0.53	0.98
Slow	1	10	0.26	0.33	0.68	1.01
Slow	4	8	0.24	0.29	0.70	0.99
		B. DNase I Digests				
Fast	1	42	0.20	0.29	0.71	1.00
Fast	3	38	0.19	0.26	0.78	1.04
Slow	1	10	0.25	0.32	0.66	0.98
Slow	4	8	0.19	0.25	0.80	1.05

[a] Results are reported as the ratio of the specific activities of repaired DNA and control DNA (σ), fraction of DNA bases in nuclease-sensitive regions (ξ), fraction of repair synthesis sites in nuclease-sensitive regions (f_S) determined from eq A6, and fraction of repair synthesis sites in nuclease-resistant regions (f_R) determined from eq A7 (see Appendix). The results for individual experiments are shown in each case.

induced DNA repair synthesis in chromatin should be examined at early (0–3 h) and late repair times (>5 h).

Staphylococcal Nuclease Digestion Kinetics. Nuclease digestion studies were performed on chromatin (nuclei) from cells labeled during replication, from cells labeled during fast repair, or from cells labeled during slow repair. Cells were labeled during replicative synthesis by adding both [^{14}C]dThd and [^{3}H]dThd during the log phase of growth and allowing the cells to come to confluence before digestion experiments were begun (see Materials and Methods). To label cells during repair synthesis, cells were prelabeled with [^{14}C]dThd during the log phase of growth and allowed to come to confluence. These cells were then exposed to UV. To label cells during fast-repair synthesis, the cells were labeled with [^{3}H]dThd during the initial 3 h after exposure (Figure 1). To label cells during slow-repair synthesis, [^{3}H]dThd was not added until 8–12 h after UV. These cells were then labeled until ~30 h after exposure. Hydroxyurea was present during repair synthesis. During the fast-repair phase at least 97% of the isotope was incorporated by repair synthesis, and during the slow repair phase at least 87% of the isotope was incorporated by repair synthesis (calculated from σ; see Table I).

Staphylococcal nuclease digestion kinetics of nuclei from cells double labeled during replication, labeled during replication and fast repair, or labeled during replication and slow repair are presented in Figure 2. The acid-soluble counts released as a function of time for each isotope are shown in Figure 2a–c, while the fraction (f) of each labeled nucleotide released is shown in Figure 2d–f. [We note that little acid-soluble material is released in the absence of nuclease (Figure 2a–c), suggesting that under our experimental conditions there is little, if any, endogenous nuclease activity present.] For cells labeled with both isotopes during replication, the functional dependences of the fraction of counts released are the same (Figure 2d). In contrast, isotope incorporated during the fast phase of repair ([^{3}H]dThd) is released more rapidly from chromatin (nuclei) than isotope incorporated during replication ([^{14}C]dThd) (Figure 2e). Isotope incorporated during slow-repair synthesis also appears to be released more rapidly from nuclei than isotope incorporated during replication, but the difference is much smaller than that seen in the case of fast repair (Figure 2f).

In order to quantitate these differences, we have developed a method of analysis which allows the determination of the fraction of repair sites (nucleotides inserted) present in nuclease-sensitive or -resistant regions in the genome (see Appendix). Experimentally, this analysis rests on comparisons of the release of isotope from chromatin (nuclei) and from its corresponding "naked" DNA. The method requires the nu-

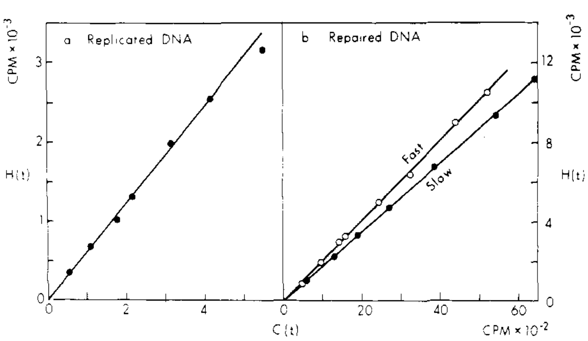

FIGURE 3: $H(t)$ vs. $C(t)$ plot for naked DNA. $H(t)$ (^{3}H cpm at time t) vs. $C(t)$ (^{14}C cpm at time t) (see Appendix) for DNA from the cells used to generate the data in Figure 2. DNA (18, 28, and 22 μg/mL for replicated, fast repair, and slow repair, respectively) was incubated with staphylococcal nuclease at a DNA-enzyme ratio of 500: replicated (a), fast repair synthesis (b, O), and slow repair synthesis (b, ●).

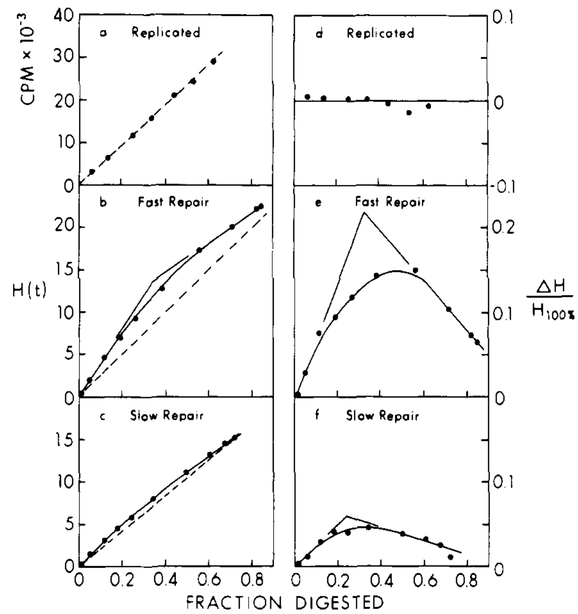

FIGURE 4: $H(t)$ vs. $C(t)$ plots and difference plots for cells labeled during replication, fast repair, and slow repair. Nuclei data (Figure 2) were plotted (●) in the same manner as described in Figure 3 (see also Appendix) and compared with the fits shown in Figure 3 for the corresponding naked DNA (dashed line) (Figure 4a–c). The abscissa has been changed from $C(t)$ to $C(t)/C_{100\%}$ (i.e., fraction of genome digested; see Results). Normalized difference plots (Figure 4d–f) were calculated from the expression:

$$\frac{\Delta H}{H_{100\%}} = \frac{H(t)_{\mathrm{CHR}} - m_{\mathrm{NAK}}C(t)_{\mathrm{CHR}}}{H_{100\%}}$$

where $H(t)_{\mathrm{CHR}} = H(t)$ for chromatin (nuclei), m_{NAK} = slope of fit to naked DNA digestion data (Figure 3), $C(t)_{\mathrm{CHR}} = C(t)$ for chromatin (nuclei), and $H_{100\%}$ = 100% digestion value of ^{3}H cpm for chromatin (Materials and Methods). DNA double labeled during replication (a, d). DNA prelabeled during replication and labeled during fast-repair synthesis (b, e). DNA prelabeled during replication and labeled during slow-repair synthesis (c, f).

clease digestion data to be plotted as the amount of [^{3}H]dThd released vs. the amount of [^{14}C]dThd released at each time point [$H(t)$ vs. $C(t)$; Appendix]. Figure 3 shows typical results for the staphylococcal nuclease digestion of naked DNA which was labeled during replication with [^{14}C]dThd and during replication or repair with [^{3}H]dThd. Not surprisingly, digestion of naked DNA labeled during replication with the two isotopes yields a straight line and indicates that both isotopes are digested at the same rate (Figure 3a). Likewise, when naked DNA from cells labeled during replicative synthesis with [^{14}C]dThd and during repair synthesis with [^{3}H]dThd are digested, straight lines are obtained (Figure 3b). These results indicate that the nuclease makes no distinction between replicated sites and repaired sites in *naked DNA* (Appendix).

The chromatin (nuclei) data in Figure 2 are plotted as $H(t)$ vs. $C(t)/C_{100\%}$ in Figure 4a–c along with the results obtained from Figure 3 for the corresponding naked DNAs. The abscissa has been modified from $C(t)$ to $C(t)/C_{100\%}$ (i.e., the fraction of the total genome) to facilitate graphic analysis of ξ (i.e., the fraction of the total genome in nuclease sensitive regions; Appendix). When plotted in this manner, the data yield curves of the type predicted by the theory (Appendix; Figure 9).

Direct comparisons between each case can be made by plotting the respective differences between chromatin and naked DNA as normalized difference plots (Figure 4d–f). As can be seen, for the replicated case the difference data form essentially a straight line about zero (Figure 4d). In contrast, the data for the fast-repair case show a marked deviation from zero (Figure 4e). The intercept of the initial and final slopes is at a fractional value of 0.32 (ξ). As discussed in the Appendix, this result indicates that approximately 30% of the genome is in staphylococcal nuclease-sensitive regions. The difference data for the slow repair case also show a deviation from zero (Figure 4f); however, the magnitude of the difference is much smaller than that seen for the fast-repair case (Figure 4e).

The data in Figure 4 were analyzed as described in the Appendix, and the results, along with results from other experiments, are shown in Table I (part A). For each experiment the DNA from control cells (unirradiated, hydroxyurea suppressed) was prepared along with the DNA from damaged cells and used to determine σ (i.e., the ratio of the specific activities). These values for σ are minimal estimates, since they have not been corrected for any UV suppression of replicative synthesis. However, it is clear from Figure 10 (Appendix) that correction of our values for σ is unnecessary. The results shown for ξ, f_S, and f_R were determined from plots like those shown in Figure 4 using eq A6 and A7 of the Appendix. In each case the data give good sum tests (Appendix). It is noted that in cases where the differences between the chromatin data and the naked DNA data are small, e.g., slow repair, a more accurate determination of ξ, f_S, and f_R can be made from the difference plot rather than a plot of $H(t)$ vs. $C(t)$. The extension of the method to this type of plot follows directly.

From Table I (part A) it can be seen that in the case of fast-repair synthesis approximately 50% of the repair sites are located in staphylococcal nuclease-sensitive regions (f_S), which comprise approximately 32% of the genome (ξ). In the case of slow-repair synthesis only about 30% of the repair sites are located in staphylococcal nuclease-sensitive regions, which comprise approximately 25% of the genome. The decrease in ξ in going from fast (32%) to slow (25%) repair digestions may represent a difference between these two repair periods in the amount of genome rendered staphylococcal nuclease sensitive but also may reflect the error in the determination of this parameter (see Smerdon and Lieberman, 1978).

Electrophoresis Resistant DNA fragments produced during staphylococcal nuclease digestions were analyzed by collecting duplicate aliquots during the course of digestion. One set was used to generate an $H(t)$ vs. $C(t)$ plot (e.g., Figure 4), while the other was used to prepare DNA fragments for electrophoresis on agarose gels. This $H(t)$ vs. $C(t)$ plot, a photograph of the gel, and gel scans are presented in Figure 5. Inspection of these data indicates that for times before the breakpoint (ξ; less than 8 min) most of the DNA bands as

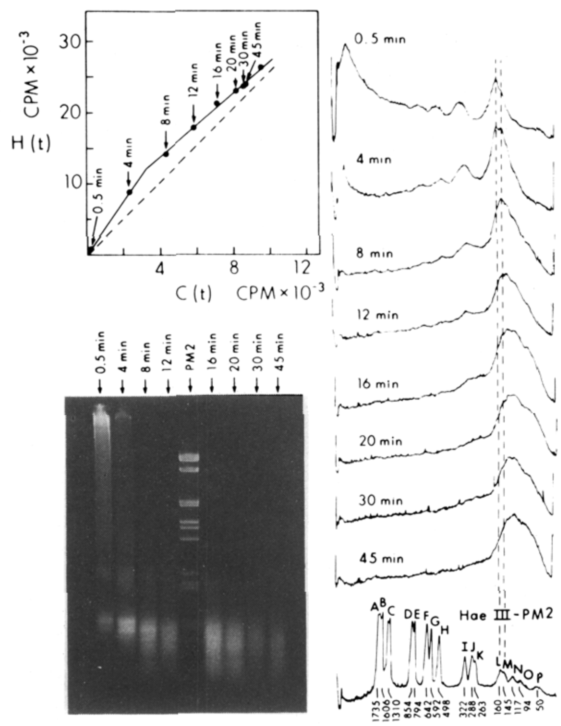

FIGURE 5: Analysis of ξ by agarose gel electrophoresis. The upper left panel is an $H(t)$ *vs.* $C(t)$ plot for cells labeled during fast-repair synthesis (●) as described in Figure 2 (1 μg/mL staphylococcal nuclease; 25–30 μg/mL DNA chromatin as nuclei). The dashed line represents fit to digestion data for the corresponding naked DNA. At the indicated times, duplicate aliquots were taken: one was used to determine the acid-soluble cpm and the other to prepare DNA for agarose gel (2.8%) electrophoresis (lower left). Direction of migration is from top to bottom. *Hae*III restriction fragments of PM2 DNA are included. The right panel represents scans of the negative. The pair of dashed lines represents the position of *Hae*III restriction fragments L and M (160 and 145 bp, respectively). Sizes shown for restriction fragments are in base pairs.

monomer (~140–160 bp), multimer, or high-molecular-weight DNA, and very little appears as submonomer fragments.[3] After the breakpoint, submonomer fragments begin to appear and eventually predominate, and very little multimer DNA is present. These results suggest that the breakpoint we observe corresponds to the point at which most of the linker DNA is digested and most of the core DNA is undigested. Thus, our values for ξ approximate the fraction of total DNA in the linker regions, and the resistant regions are comprised primarily of core particles.

The size of the linker regions in the human genome was estimated by measuring the repeat length at different digestion times (Lohr et al., 1977). We obtained a repeat length of 193 bp and, using 145 bp as the monomer length, a maximum average linker size of 48 bp which approached 0 bp at long digestion times (data not shown).

To complement our analysis of nuclease-sensitive regions, we examined the distribution of repair synthesis in nuclease-resistant regions by agarose gel electrophoresis. In this procedure, nuclei labeled by replication, fast- or slow-repair synthesis (see legend to Figure 2), were digested with staphylococcal nuclease, and the DNA was electrophoresed and counted (Figure 6). In each case, the ^3H and ^{14}C profiles are shown as a function of migration into the gel (Figure 6b,d,f,g)

[3] Closer inspection of the gel pattern reveals that the monomer region is actually composed of a doublet, one band consisting of ~160 bp of DNA and the other consisting of ~145 bp of DNA. Initially, the 160-bp band predominates; with digestion, this band diminishes while the relative proportion of the 145-bp band increases.

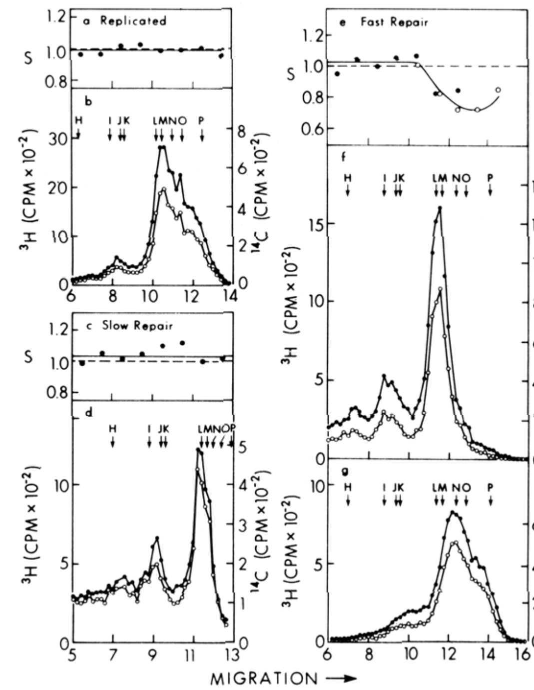

FIGURE 6: Electrophoretic analysis of staphylococcal nuclease-resistant regions of chromatin. Panels b, d, f, and g present agarose gel profiles of DNA prepared after nuclease digestion of nuclei (^3H cpm, ●; ^{14}C cpm, ○). Panel b depicts a profile of DNA from cells double labeled during replication; nuclei were digested for 4 min at a concentration of 400 μg/mL DNA chromatin and 10 μg/mL nuclease (see Materials and Methods for details). Panel d depicts a profile of DNA from cells prelabeled during replication (^{14}C) and labeled during slow-repair synthesis (^3H); nuclei were digested for 45 min at a concentration of 30 μg/mL DNA chromatin and 0.1 μg/mL nuclease. Panels f and g depict similar profiles from cells prelabeled during replication (^{14}C) and labeled during fast-repair synthesis (^3H); nuclei were digested for 4 (panel f) and 16 min (panel g) at a concentration of 30 μg/mL DNA chromatin and 1 μg/mL nuclease. Arrows represent the position of *Hae*III restriction fragments (Figure 5). Panels a, c, and e represent the ^3H to ^{14}C ratios normalized to the ^3H to ^{14}C ratio of undigested DNA (S). Panel a presents values for S for the gel profile in panel b; panel c presents S for panel d; panel e presents S for panels f (●), and g (○). S represents values averaged over five 2-mm sections. The solid line is a fit to the data, and the dashed line is the value for undigested DNA.

along with the position of the PM2 marker fragments. Above each gel profile is shown the relative specific activity (i.e., the ^3H to ^{14}C ratio normalized to the ^3H to ^{14}C ratio for the respective purified undigested DNA) as a function of distance migrated (Figure 6a,c,e). The relative specific activities of the replicated DNA fragments show very little deviation from unity and indicate that the distribution of replicated sites in core particles is the same as the genome as a whole (Figure 6a). In the case of fast-repair synthesis, however, there is a marked decrease in repair counts in monomer DNA (Figure 6e), indicating that there is less repair synthesis in core particle regions than in the genome as a whole. In the case of slow-repair synthesis, this marked decrease in relative specific activity is not seen (Figure 6c).

DNase I Digestions. The three different classes of nuclei were also digested with DNase I (Figures 7 and 8). As was seen in staphylococcal nuclease digestion studies, isotope incorporated during fast- and slow-repair synthesis is released more rapidly by DNase I than is isotope incorporated by replicative synthesis (Figure 7). However, in the case of fast-repair synthesis a smaller fraction of the repair counts is released by DNase I after long digestion times (~75%) than by staphylococcal nuclease (>95%) (compare Figures 2e and 7b). Also, similar digestion curves are obtained for fast- and slow-repair

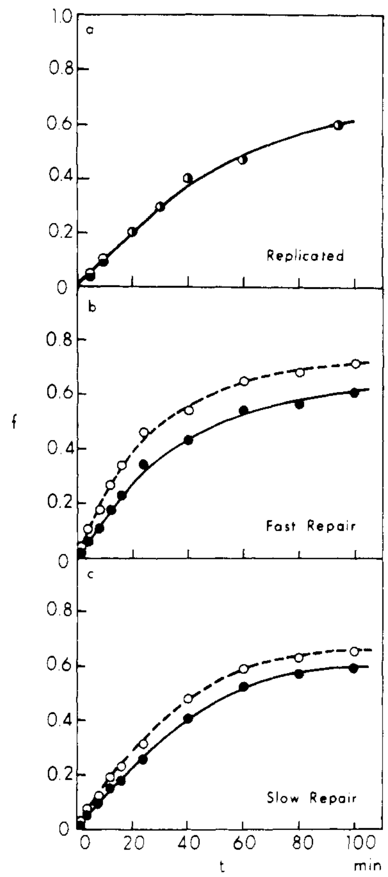

FIGURE 7: DNase I digestion kinetics for nuclei labeled during replication, fast repair, and slow repair. The fractions (f) of ^3H (O) and ^{14}C cpm (●) released as a function of time (t) are presented for nuclei double labeled during replication (a), prelabeled during replication (^{14}C) and labeled during fast-repair synthesis (^3H) (b), and prelabeled during replication (^{14}C) and labeled during slow-repair synthesis (^3H) (c). The nuclei used for these studies and those in Figure 2 were from the same preparations. The DNase I concentration was 0.4 μg/mL, and the nuclei concentrations were the same as those given in Figure 2.

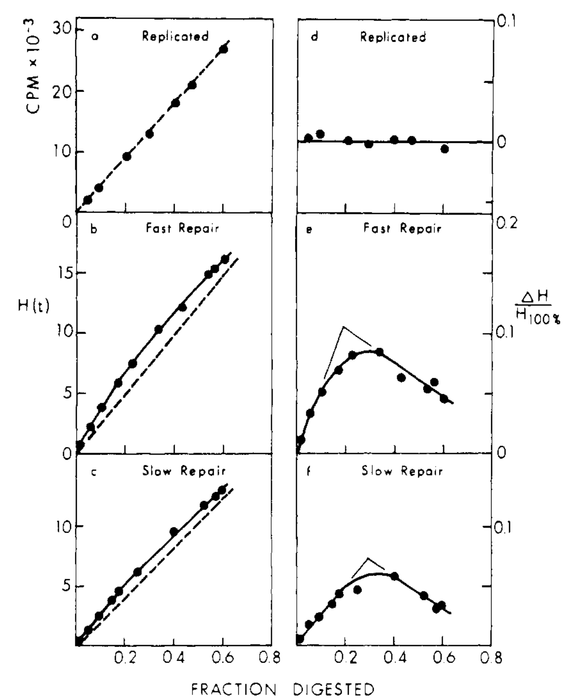

FIGURE 8: $H(t)$ vs. $C(t)$ plots and difference plots for cells labeled during replication, fast repair, and slow repair. The data in Figure 7 are plotted as described in the legend to Figure 4: replicated, a and d; fast repair synthesis, b and e; slow repair synthesis, c and f.

synthesis studies when $H(t)$ vs. $C(t)$ plots and difference plots are generated (Figure 8). This finding contrasts with the staphylococcal nuclease digestion studies (compare Figures 4 and 8).

Table I (part B) presents the calculated values of σ, ξ, f_S, and f_R for DNase I digestions. For the fast-repair case, approximately 28% of the repair sites (f_S) and approximately 20% of the genome (ξ) are in DNase I sensitive regions. These values are in marked contrast to those obtained for staphylococcal nuclease (50 and 32%, respectively). In the slow-repair case, however, the values obtained for DNase I ($f_S \simeq 0.29$ and $\xi \simeq 0.22$) are similar to those obtained for staphylococcal nuclease ($f_S \simeq 0.31$ and $\xi \simeq 0.25$). This result is surprising in view of the fact that DNase I and staphylococcal nuclease appear to cleave chromatin at different sites (see introductory statement). At present, we do not know the significance of this finding.

Discussion

Our data provide evidence that the structural constraints placed upon DNA in chromatin also place constraints on the distribution of DNA repair synthesis after treatment of human fibroblasts with ultraviolet radiation. Of interest is the observation that repair synthesis occurring soon after damage differs from that seen at more extended times not only in the rate of nucleotide incorporation but also in the distribution of repair synthesis within chromatin.

The time course of repair synthesis following UV was measured by different techniques, each involving different assumptions and methodology. With each of these methods a rapid phase was distinguishable from a slow phase; during the fast phase, nucleotides are inserted about 12 times more rapidly than during the slow phase. In agreement with our findings, previous studies of UV and ionizing radiation-induced repair synthesis in human cells have demonstrated two discrete phases (Spiegler and Norman, 1969, 1970; Connor and Norman, 1971; Edenberg and Hanawalt, 1973). In addition, Amacher et al. (1977) have provided evidence that, like repair synthesis, pyrimidine dimer removal has a rapid component. A number of factors in addition to chromatin structure (see next two paragraphs) may be related to our findings: (1) Fast- and slow-repair synthesis may represent repair synthesis associated with the removal of different UV-induced lesions; (2) the average patch size may be different during the fast and slow phases so that the *actual rates of removal of damage* may be similar, but the *apparent rates of repair synthesis* on a unit DNA basis are different; (3) UV damage may be repaired by two (or more) repair systems in human cells—one of which is rapid while the other is an order of magnitude slower. Clearly, these possibilities are not mutually exclusive.

Studies of the staphylococcal nuclease sensitivity of nucleotides inserted during fast and slow repair allow inferences about the distribution of repair synthesis within chromatin. Our data (Table I) indicate that during fast-repair synthesis approximately 50% of the repair sites occur in rapidly digestible regions of the genome which together comprise only about 30% of the nuclear DNA. Therefore, on a unit DNA basis, the amount of repair synthesis occurring in nuclease-sensitive regions of the genome (f_S/ξ) is approximately twice that of the amount in resistant regions [$f_R/(1-\xi)$]. Furthermore, specific-activity measurements of DNA fragments separated by gel electrophoresis confirm the relative underrepresentation of fast-repair synthesis in nuclease-resistant regions (core particles; Figure 6e). In contrast, repair synthesis which occurs during slow repair is more uniformly distributed throughout the genome.

Although staphylococcal nuclease preferentially digests linker regions of nucleosomes, we also find that a certain fraction of 160-bp monomer-associated DNA is more sensitive to nuclease than the 145-bp monomer DNA and submonomer fragments. It is also likely that regions of the genome not packaged as nucleosomes are relatively nuclease sensitive (e.g., ribosomal cistrons; Foe, 1977). However, because our analysis utilizes the intercept of the *initial* and final slopes for the determination of ξ (e.g., Figure 4), the nuclease-sensitive regions, as defined in this communication, are composed primarily of linker regions (Figure 5). This conclusion is supported by the fact that the initial repeat length of 193 bp, with average linker size of 48 bp, yields a value of 0.25 for the fraction of the genome in linker regions if the entire genome is packaged as nucleosomes. This fractional value is similar to our determinations of ξ (0.25–0.32).

A number of possibilities could account for our results. It is not clear, for example, whether damage (i.e., pyrimidine dimers and other UV photoproducts) is uniformly distributed throughout the genome or shows a preferential distribution within chromatin. Thus, the preferential repair synthesis seen in linker regions during fast repair may be reflective of: (1) nonuniform distribution of damage, (2) the ease of access to uniformly distributed damaged sites by a single repair process, or (3) different repair processes acting in different regions of chromatin. In the case of slow repair, the long labeling times used to obtain sufficient incorporation of [^{3}H]dThd might allow some redistribution of chromosomal proteins with respect to repaired sites. Thus, another possibility which might account, at least in part, for our results is movement of histone cores along the DNA strand ("sliding"). Finally, it is possible that the repair process does not completely restore all regions of chromatin to their original (undamaged) structures, thereby yielding these regions more (or less) susceptible to nuclease digestion. Clearly, these and other possibilities require experimental examination. However, the finding of preferential repair synthesis in nuclease-sensitive regions of chromatin during fast repair is of interest in view of previous observations that the complexity of DNA itself does not appear to be related to the distribution of repair synthesis (Meltz and Painter, 1973; Lieberman and Poirier, 1974a,b; Drahovsky et al., 1976).

The DNase I results are more difficult to interpret because less is known about the sensitivity of regions of DNA in chromatin to this enzyme. During both fast- and slow-repair synthesis there is an enhancement of repair sites in nuclease-sensitive regions. This difference is not as dramatic as that seen with staphylococcal nuclease and fast repair (compare Figure 4 with Figure 8). In addition, the fraction of repair sites in DNase I sensitive regions is approximately the same for fast and slow repair. This finding also contrasts with staphylococcal nuclease studies. Although DNase I is known to digest preferentially regions of chromatin which are being actively transcribed (Weintraub and Groudine, 1976; Garel and Axel, 1976; Levy and Dixon, 1977), it is not clear what fraction of the total DNase I sensitive sites is represented by these genes. As a result, no definitive statement can be made about preferential repair of active genes. The contrast between the results obtained with staphylococcal nuclease and those obtained with DNase I demonstrates that the findings are specific and related to distinctive features of chromatin structure.

While this manuscript was in preparation, Cleaver (1977) reported similar results using staphylococcal nuclease. He demonstrated that the fraction of repair synthesis sites in nuclease-sensitive DNA is greater for repair synthesis occurring during the first 10 min after UV damage than during the first 30 min after damage. Using our method, we also find a marked increase in the fraction of repair sites in staphylococcal nuclease-sensitive regions (f_S/ξ) for very early repair times (Smerdon and Lieberman, 1978). Another study has suggested that following treatment of mouse mammary cells with methyl methanesulfonate repair synthesis occurs in staphylococcal nuclease-sensitive regions (Bodell, 1977). In addition, Ramanthan et al. (1976) have demonstrated preferential removal of damage (dimethylnitrosamine-induced) from rat liver chromatin by DNase I and staphylococcal nuclease. These results are in general agreement with our findings.

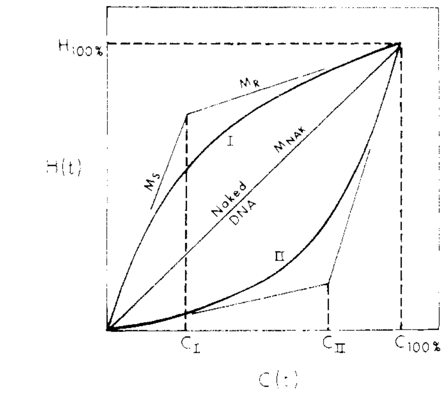

FIGURE 9: Hypothetical $H(t)$ vs. $C(t)$ curves for nuclease digestion of chromatin. $H_{100\%}$ = 100% digestion value for $H(t)$ (i.e., repaired DNA); $C_{100\%}$ = 100% digestion value for $C(t)$ (i.e., total genome); m_S = initial slope; m_R = final slope; m_{NAK} = slope of line generated by digestion of naked DNA (eq A3); C_I = value of $C(t)$ at intercept of initial and final slopes for curve I; and C_{II} = value of $C(t)$ at intercept of initial and final slopes for curve II.

A number of methodological considerations require comment. A major feature of our analysis is that it allows specification of the fraction of repair sites in nuclease-sensitive and -resistant regions. These estimates cannot be obtained from fractional digestion curves alone (e.g., Figure 2), because it is clear that these curves are the result of digestion of at least two different regions of chromatin with differing nuclease sensitivities (e.g., Figure 5). Related to this problem is our observation that the fraction of the genome which is digested (^{14}C-cpms; limit digest) is greater in irradiated cells than in unirradiated cells (Figure 2d,e). While the reason for this increased sensitivity is unknown, it is still possible to quantitate the distribution of repair sites (f_S) by our method (Appendix). We also note that even for low levels of repair synthesis our method of analysis is applicable (Figure 10). This observation may be relevant in view of the fact that it is sometimes difficult to obtain as much repair synthesis after damage with chemical carcinogens as that seen following UV. Although we have developed the analysis to examine the distribution of repair synthesis, there is no reason why, in principle at least, it is not applicable to other repair phenomena (e.g., removal of damage).

We have used a confluent cell–hydroxyurea suppression system to obtain nuclei in which most of the label is incorporated during repair synthesis. The validity of this approach is borne out both by our own data and by those in the literature. Our results (Figure 1) indicate that the time course of repair synthesis is essentially the same, whether measured with hydroxyurea-suppressed cells or with cells in which BrdUrd is used to shift the density of newly replicated DNA (no hydroxyurea). These findings are in agreement with those of Smith and Hanawalt (1976a). A number of other studies have found little, if any, difference between hydroxyurea-treated cells and untreated cells, either in the amount of repair synthesis (Evans and Norman, 1968; Robbins and Kraemer, 1972; Painter et al., 1973; Ikenaga and Kakunaga, 1977) or in the extent of damage removed (Ikenaga and Kakunaga, 1977; Ikenaga et al., 1977). Smith and Hanawalt (1976a) did find a 25–40% increase in the estimate of the amount of repair synthesis in growing (WI-38) and transformed cells (VA-13) when hydroxyurea was present; however, this difference was not observed when confluent cells (WI-38) were used.

Acknowledgments

We thank Drs. R. T. Kovacic and K. E. Van Holde for providing the *Hae*III restriction fragments of PM2 DNA used as markers for the electrophoretic analyses, Dr. John Newbold for the electrophoresis apparatus, and Mrs. J. L. Belanger for her skillful technical assistance.

Appendix

Based on the work of others, as well as our own results, the different structural regions of chromatin can be approximated as nuclease sensitive or nuclease resistant. Using this simplified representation of chromatin structure, one can quantitate the distribution of repair synthesis sites between the two different regions in the following way: Let S and R be the number of DNA bases incorporated by repair synthesis in nuclease-sensitive and -resistant regions, respectively; s and r be the number of DNA bases incorporated by replicative synthesis during the period of repair synthesis in nuclease-sensitive and -resistant regions, respectively; and $H(t)$ be the total number of repaired and newly replicated bases digested by nuclease after time t. Therefore,

$$H(t) = (S + s)\alpha(t) + (R + r)\beta(t)$$

where $\alpha(t)$ = fraction of S and s digested by time t, and $\beta(t)$ = fraction of R and r digested by time t.

Also, if we let L and M be the total number of DNA bases in nuclease-sensitive and -resistant regions, respectively, and $C(t)$ be the total number of DNA bases digested by nuclease after time t, then

$$C(t) = L\alpha(t) + M\beta(t)$$

If the rate of digestion of nuclease-sensitive regions is much larger than the rate of digestion of nuclease resistant regions, then for early times

$$H(t) \simeq (S + s)\alpha(t)$$

and

$$C(t) \simeq L\alpha(t)$$

From these,

$$H(t) = \left(\frac{S + s}{L}\right) C(t) \tag{A1}$$

Similarly, for long times $\alpha(t) \simeq 1$ and

$$H(t) = \left(\frac{R + r}{M}\right) C(t) + \phi \tag{A2}$$

where

$$\phi = S + s - \left(\frac{R + r}{M}\right) L$$

Also, for the purified "naked" DNA, assuming $\alpha(t) = \beta(t)$,

$$H(t) = \left(\frac{S + s + R + r}{L + M}\right) C(t) \tag{A3}$$

Therefore, if one plots $H(t)$ vs. $C(t)$ for repaired chromatin and its naked DNA, the ratio (η_S) of the *initial* slope of the chromatin data and the slope of the naked DNA data is, from eq A1 and A3,

$$\eta_S = \frac{f_S\left(\frac{S + R}{s + r}\right) + a}{\xi\left(\frac{S + R}{s + r} + 1\right)}$$

where $f_S = S/(S + R)$ = fraction of repair synthesis sites in the nuclease-sensitive regions; $\xi = L/(L + M)$ = fraction of DNA bases in the nuclease-sensitive regions; $a = s/(s + r)$ = fraction of newly replicated sites in the nuclease-sensitive regions. If one assumes that the newly replicated regions have no preference for sensitive or resistant regions (which is easily measurable), then $a = \xi$, and

$$\eta_S = \frac{f_S\left(\frac{S + R}{s + r}\right) + \xi}{\xi\left(\frac{S + R}{s + r} + 1\right)} \tag{A4}$$

Similarly, the ratio (η_R) of the *final* slope of the chromatin data and the slope of the naked DNA data is, from eq A2 and A3,

$$\eta_R = \frac{f_R\left(\frac{S + R}{s + r}\right) + (1 - \xi)}{(1 - \xi)\left(\frac{S + R}{s + r} + 1\right)} \tag{A5}$$

where $f_R = R/(S + R)$ = fraction of repair synthesis sites in the nuclease-resistant regions. Now, the ratio of the specific activities (σ) of the purified repaired DNA and the purified control DNA (from cells treated identically as the repaired cells without irradiation), is

$$\sigma = \frac{S + R}{s + r} + 1$$

Therefore, from eq A4 and A5,

$$f_S = \frac{(\eta_S\sigma - 1)}{\sigma - 1}\xi \tag{A6}$$

and

$$f_R = \frac{(\eta_R\sigma - 1)}{\sigma - 1}(1 - \xi) \tag{A7}$$

From eq A6 and A7 the fraction of repair-synthesis sites in the nuclease-sensitive and -resistant regions can be determined independently from the same data (provided the digestion conditions are such that a good determination of the initial and final slopes can be made). Since the sum of these two fractions must be unity, this method provides a natural test for the values that one obtains and for the validity of the assumptions made. Thus, we refer to the sum of f_S and f_R as the "sum test".

In order to understand better the method for determining η_S, η_R, and ξ, it is helpful to consider the hypothetical curves in Figure 9. The figure shows three possible dependencies of $H(t)$ on $C(t)$ (labeled I, II, and "Naked DNA") for the digestion of chromatin with nuclease. The "Naked DNA" line (with slope m_{NAK}) is so labeled, since it is also the line gener-

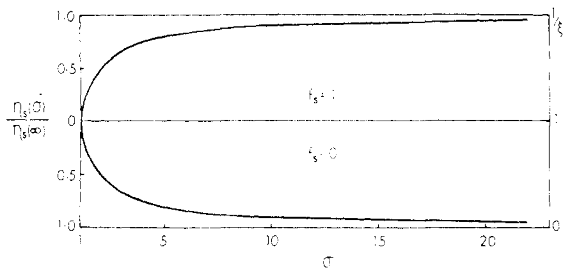

FIGURE 10: Dependence of η_S on σ. η_S (right ordinate) and $\eta_S(\sigma)/\eta_S(\infty)$ (the fraction of maximum η_S; left ordinate) as a function of σ are presented for $f_S = 1$ and $f_S = 0$ (see eq A6).

ated by a digestion of the purified DNA and is defined by eq A3. If the chromatin digestion data falls on this line, $\eta_S = \eta_R = 1$. This indicates that the number of repair sites per unit DNA is the same in the nuclease-sensitive and -resistant regions. If the chromatin data fall on a curve above the naked DNA line, such as curve I, then $\eta_S > 1$ and there is a preference of repair sites for the nuclease-sensitive regions. Similarly, a curve below the naked DNA line, such as curve II, suggests a preference for resistant regions. For curve I, the initial slope m_S and the final slope m_R have an intercept at C_I. Therefore, $\eta_S = m_S/m_{NAK}$, $\eta_R = m_R/m_{NAK}$, and $\xi = C_I/C_{100\%}$. (The determination of $C_{100\%}$ is discussed under Materials and Methods.) Similar expressions can be written for curve II.

The sensitivity of this type of analysis is indicated in Figure 10. The figure shows the dependence of the minimum ($f_S = 0$) and the maximum ($f_S = 1$) values of η_S on σ. It can be seen that η_S rapidly approaches $1/\xi$ for $f_S = 1$ and 0 for $f_S = 0$. This is an important advantage of the method, since only a small fraction of the DNA is damaged or repaired in any given experiment, and thus the number of counts in the repaired cells may only be five to ten times greater than the number of counts in the control. Even for a σ of 5, there is an appreciable difference between the maximum and minimum values of η_S.

References

Amacher, D. E., Elliott, J. A., and Lieberman, M. W. (1977), *Proc. Natl. Acad. Sci. U.S.A. 74*, 1553–1557.

Axel, R., Ceder, H., and Felsenfeld, G. (1975), *Biochemistry 14*, 2489–2495.

Beers, R. F., Harriott, R. M., and Tilghman, R. C., Ed. (1972), Molecular and Cellular Repair Processes, Baltimore, Md., Johns Hopkins University Press.

Bodell, W. J. (1977), *Nucleic Acids Res. 4*, 2619–2628.

Cleaver, J. E. (1974), *Adv. Radiat. Biol. 4*, 1–75.

Cleaver, J. E. (1977), *Nature (London) 270*, 451–453.

Conner, W. G., and Norman, A. (1971), *Mutat. Res. 13*, 393–402.

Drahovsky, D., Lacko, I., and Wacker, A. (1976), *Biochim. Biophys. Acta 447*, 139–143.

Edenberg, H. J., and Hanawalt, P. C. (1973), *Biochim. Biophys. Acta 324*, 206–217.

Evans, R. G., and Norman, A. (1968), *Radiat. Res. 36*, 287–298.

Foe, V. E. (1977), *Cold Spring Harbor Symp. Quant. Biol. 42*, in press.

Garel, A., and Axel, R. (1976), *Proc. Natl. Acad. Sci. U.S.A. 73*, 3966–3970.

Hanawalt, P. C., and Setlow, R. B., Ed. (1975), *Basic Life Sci. 5*.

Hewish, D. R., and Burgoyne, L. A. (1973), *Biochem. Biophys. Res. Commun. 52*, 504–510.

Horrocks, D. L., Ed. (1974), Applications of Liquid Scintillation Counting, New York, N.Y., Academic Press.

Ikenaga, M., and Kakunaga, T. (1977), *Cancer Res. 37*, 3672–3678.

Ikenaga, M., Takebe, H., and Ishii, Y. (1977), *Mutat. Res. 43*, 415–427.

Keichline, L. D., Villee, C. A., and Wassarman, P. M. (1976), *Biochim. Biophys. Acta 425*, 84–94.

Kobayashi, Y., and Maudsley, D. V., Ed. (1974), Biological Applications of Liquid Scintillation Counting, New York, N.Y., Academic Press.

Kornberg, R. D. (1974), *Science, 184*, 868–871.

Kovacic, R. T., and Van Holde, K. E. (1977), *Biochemistry 16*, 1490–1498.

Lacy, E., and Axel, R. (1975), *Proc. Natl. Acad. Sci. U.S.A. 72*, 3978–3982.

Levy, B. W., and Dixon, G. H. (1977), *Nucleic Acids Res. 4*, 883–898.

Lieberman, M. W. (1976), *Int. Rev. Cytol. 45*, 1–23.

Lieberman, M. W., and Dipple, A. (1972), *Cancer Res. 32*, 1855–1860.

Lieberman, M. W., and Poirier, M. C. (1973), *Cancer Res. 33*, 2097–2103.

Lieberman, M. W., and Poirier, M. C. (1974a), *Biochemistry 13*, 3018–3023.

Lieberman, M. W., and Poirier, M. C. (1974b), *Proc. Natl. Acad. Sci. U.S.A. 71*, 2461–2465.

Lieberman, M. W., and Poirier, M. C. (1974c), *Biochemistry 13*, 5384–5388.

Lohr, D., Corden, J., Tatchell, K., Kovacic, R. T., and Van Holde, K. E. (1977), *Proc. Natl. Acad. Sci. U.S.A. 74*, 79–83.

Meltz, M. L., and Painter, R. B. (1973), *Int. J. Radiat. Biol. 23*, 637–640.

Nichols, W. W., and Murphy, D., Ed. (1977), DNA Repair Processes, Miami, Fla., Symposia Specialists.

Nichols, W. W., Murphy, D. G., Cristofalo, V. J., Toji, L. H., Greene, A. E., and Dwight, S. A. (1977), *Science 196*, 60–63.

Noll, M. (1974), *Nature (London) 251*, 249–251.

Olins, A. L., and Olins, D. E. (1973), *J. Cell Biol. 59*, 252a.

Olins, A. L., and Olins, D. E. (1974), *Science 183*, 330–332.

Painter, R. B., Clarkson, J. M., and Young, B. R. (1973), *Radiat. Res. 56*, 560–564.

Ramanathan, R., Rajalakshmi, S., Sarma, D. S. R., and Farber, E. (1976), *Cancer Res. 36*, 2073–2079.

Robins, J. A., and Kraemer, K. H. (1972), *Biochim. Biophys. Acta 227*, 7–14.

Sahasrabuddhe, C. G., and Van Holde, K. E. (1974), *J. Biol. Chem. 249*, 152–156.

Simpson, R. T., and Whitlock, J. P. (1976), *Cell 9*, 347–353.

Smerdon, M. J., and Lieberman, M. W. (1978), in DNA Repair Mechanisms, Hanawalt, P. C., Friedberg, E. C., and Fox, C. F., Eds., New York, N.Y., Academic Press, in press.

Smith, C. A., and Hanawalt, P. C. (1976a), *Biochim. Biophys. Acta 432*, 336–347.

Smith, C. A., and Hanawalt, P. C. (1976b), *Biochim. Biophys. Acta 447*, 121–132.

Spiegler, P., and Norman, A. (1969), *Radiat. Res. 39*, 400–412.

Spiegler, P., and Norman, A. (1970), *Radiat. Res. 43*, 187–195.

Weintraub, H., and Groudine, M. (1976), *Science 193*, 848–856.

Woodcock, C. L. F. (1973), *J. Cell Biol. 59*, 368a.